Brazilian Journal
of Chemical
Engineering

ISSN 0104-6632
Printed in Brazil

Vol. 21, No. 04, pp. 667 - 680, October - December 2004

MASS TRANSPORT IN SPHEROIDS USING THE GALERKIN METHOD

D. R. Lima, S. N. Farias and A. G. B. Lima*

Centro de Ciências e Tecnologia, Departamento de Engenharia Mecânica,
Universidade Federal de Campina Grande, UFCG,
Phone +(55) (83) 3101317, Fax +(55) (83) 3101272,
Cx. P. 10069, CEP 58109-970, Campina Grande - PB, Brazil,
E-mail: gilson@dem.ufcg.edu.br,

(Received: October 15, 2003 ; Accepted: July 6, 2004)

Abstract - This work presents an analytical modelling of mass transfer in spheroidal solids using a liquid diffusion model. The diffusion equation, written in cylindrical coordinates, is solved using the Galerkin method with a constant diffusion coefficient and an equilibrium boundary condition at the surface of the solid. Results on the drying kinetics, and moisture content distribution in the solids are presented and analysed. The iso-concentration lines for moisture content show that the drying process is faster in sharp areas,. It was verified that solids with a larger area/volume ratio dry faster. The results obtained are consistent so the model presented can be used to solve diffusion problems such as drying, wetting, heating and cooling of solids with a shape that varies from a circular disk to an infinite cylinder, including a sphere and ellipsoids.
Keywords: drying, spheroid, ellipsoid, modelling, Galerkin method.

INTRODUCTION

In the chemical industries, drying is one of the most important processes used in the processing of foods and in the storage of grains. This process consists of the partial transfer of the liquid part (usually water) of a solid. The drying process can also be explained as a process of heat and mass transfer that generates the removal through evaporation of part of the moisture contained in the product (Fortes, 1978). Drying differs from other separation techniques due to the movement of the molecules, which in this case is obtained by a mass transfer of the liquid due to the difference in partial pressure of the steam between the surface of the solid to be evaporated and the air that surrounds it. In the case of foods, water is removal from the moist material up to a level where deterioration provoked by microorganisms can be minimised.

The mechanisms of moisture transport in solids are still not very well understood by specialists. Some authors consider moisture transport to be a combination of moisture transport of liquid and of vapour diffusion, while others just consider it to be liquid diffusion.

Analytical or numerical solutions of the diffusion equation, with either a constant or a variable diffusion coefficient and constant or convective boundary conditions, for several shapes (plate, cylinder and sphere), can be found in Crank (1992) and Gebhart (1993). For bodies in an elliptic shape Payne et al. (1986), Elvira (1990), Haghighi et al. (1990), Lu and Siebenmorgen (1992), Sarker et al. (1994), Lima (1999) and Lima and Nebra (2000) can be mentioned. Besides these studies, and the work of Keltner (1973), Sheen and Hayakawa (1992), Coutelieris et al. (1995), Feng and Michaelides (1997), Alassar (1999), Igathinathane and Chattopadhyay (2000), Carmo (2000), Carmo and Lima (2000, 2001), Oliveira and Lima (2001), Oliveira (2001) and Lima et al. (2002a-b) can also be mentioned.

*To whom correspondence should be addressed

Payne et al. (1986) present a solution of the heat conduction equation for an irregular border using the Galerkin method with an equilibrium boundary condition at the surface of the solid. The method was used to determine the temperature at the center of spheroids. The numerical results obtained are compared with the analytical data reported by Haji-Sheikh and Sparrow (1966), showing excellent agreement.

Lima (1999) conducted a numerical and analytical study of the heat and mass diffusion in prolate spheroids with constant or variable properties and constant or convective boundary conditions, with or without shrink, using techniques of finite volume and separation of variables. The models presented are general and independent of the nature of the solid (fruits, cereals, etc); however, the author emphasised the drying of bananas.

Oliveira and Lima (2002) offer an analytical solution of the diffusion equation applied to ellipsoids of revolution that is more than general that presented by Haji-Sheikh and Sparrow (1966). The authors included calculation of the average value of the variable of interest (moisture content) to describe mass transfer in prolate spheroids, assuming convective boundary conditions at the surface of the solid.

The goal of this research is to present an analytical methodology to predict mass transport in ellipsoids of revolution (prolate and oblate spheroids) using the Galerkin method.

MATHEMATICAL MODELLING

The general diffusion equation is given by

$$\frac{\partial(\lambda\Phi)}{\partial t} = \nabla\cdot\left(\Gamma^{\Phi}\nabla\Phi\right) + \Phi''' \tag{1}$$

By writing Eq. (1) in cylindrical coordinates, for the two-dimensional case we have

$$\frac{\partial(\lambda\Phi)}{\partial t} = \frac{1}{r}\frac{\partial}{\partial r}\left(\Gamma^{\Phi}\frac{\partial\Phi}{\partial r}\right) + \frac{\partial}{\partial z}\left(\Gamma^{\Phi}\frac{\partial\Phi}{\partial z}\right) + \Phi''' \tag{2}$$

For solution of Eq. (2), the following initial and boundary conditions can be used:

$$\Phi = \Phi(r,z) \text{ for } t = 0 \tag{3a}$$

$$\Phi = \Phi_e \text{ at the surface of the solid for } t > 0 \tag{3b}$$

$$\frac{\partial\Phi}{\partial z} = 0 \text{ for r = 0 for every } t \tag{3c}$$

$$\frac{\partial\Phi}{\partial r} = 0 \text{ for z = 0 for every } t \tag{3d}$$

Defining the following dimensionless parameters:

$$r^* = \frac{r}{a};\qquad z^* = \frac{z}{a};\qquad V^* = \frac{V}{a^3};$$

$$\Phi^* = \frac{\Phi - \Phi_e}{\Phi_0 - \Phi_e};\qquad t^* = \frac{\left(\Gamma^{\Phi}/\lambda\right)t}{a^2} \tag{4a-e}$$

Considering constant transport coefficient, without the generation of the variable, the diffusion equation assumes dimensionless form as follows:

$$\frac{\partial\Phi^*}{\partial t^*} = \nabla^2\Phi^* \tag{5}$$

In Eqs. (4a-e), " a" is a characteristic dimension of the solid.

The solution of Eq. (5) can be written as follows (Payne et al., 1986):

$$\Phi^*\left(r^*, z^*, t^*\right) = \sum_{n=1}^{N} C_n\psi_n\left(r^*, z^*\right)e^{-\gamma_n t^*} \tag{6}$$

where γ_n is the n^{th} eigenvalue (for all positions in the solid) and C_n is a constant to be determined. For convenience it is assumed that the solid has finite dimensions.

Using the integral method based on Galerkin (GBI method) (Beck et al., 1992), function $\psi_n(r^*, z^*)$ is selected so the homogeneous boundary conditions are satisfied and Eq. (6) is the solution of Eq. (5). This last condition is satisfied by substituting Eq. (6) into Eq. (5). Then, after the substitution and a series of algebraic operations, we obtain

$$\nabla^2\psi_n\left(r^*, z^*\right) + \gamma_n\psi_n\left(r^*, z^*\right) = 0 \tag{7}$$

Thus the diffusion equation will be now an eigenvalues problem and function $\psi_n(r^*, z^*)$ is the eigenfunction. Function $\Psi_n\left(r^*, z^*\right)$ is obtained by

the linear combination of a set of functions. Its members are linearly independent, so the boundary condition imposed is satisfied. This function is given by:

$$\Psi_n\left(r^*,z^*\right)=\sum_{n=1}^{N} d_{nj} f_j\left(r^*,z^*\right) \tag{8}$$

where $f_j\left(r^*,z^*\right)$ is an element of a group of base functions and d_{nj} are constants to be determined.

Function f_j is called the Galerkin function and it is obtained by the multiplication of function $\varphi\left(r^*,z^*\right)$ by an element of a complete set of functions. Function $\varphi\left(r^*,z^*\right)$ is selected so as to satisfy the homogeneous boundary condition. Function f_j with j varying from 1 to N constitutes a set of base functions.

The method to select base functions for boundary conditions of the first kind (the equilibrium boundary condition at the surface of the body) is given in the literature (Kantorovich and Krylov, Ozisik, Hagi-Sheikh and Mashena, mentioned by Beck et al., 1992). Each base function should tend towards zero at the boundary of the solid. Some, but not all, of the base functions can be zero at some point in the solid.

Using the Galerkin procedure, which consists of multiplying both sides of Eq. (7) by $f_i dV^*$ and integrating the resulting function into the volume of the solid, the following is obtained:

$$\int_{V^*} f_i \nabla^2 \Psi_n dV^* + \gamma_n \int_{V^*} f_i \Psi_n dV^* = 0 \tag{9}$$

Substituting, the Eq. (8) into Eq. (9) and dividing by the volume of the solid, we obtain:

$$\sum_{j=1}^{N} dn_j \left[\frac{1}{V^*} \int_{V^*} f_i \nabla^2 f_j dV^* + \gamma_n \frac{1}{V^*} \int_{V^*} f_i f_j dV^* \right] = 0 \tag{10}$$

where i=1,2,... ,N. In the form of the matrix, Eq. (10) can be rewritten as follows:

$$\left(\overline{A} + \gamma_n \overline{B}\right)\tilde{d}_n = 0 \tag{11}$$

where $\overline{A}$ and $\overline{B}$ are square matries of N N elements. The elements of the matries $\overline{A}$ and $\overline{B}$ are given by

$$a_{ij} = \frac{1}{V^*} \int_{V^*} f_i \nabla^2 f_j dV^* \tag{12a}$$

$$b_{ij} = \frac{1}{V^*} \int_{V^*} f_i f_j dV^* \tag{12b}$$

Coefficients $d_{n1}, d_{n2}, \ldots, d_{nN}$ in Eq. (8) are elements of vector $\tilde{d}_n$ in Eq. (11). It can be observed that matrix $\overline{B}$ is symmetrical, so $b_{ij} = b_{ji}$. Matrix $\overline{A}$ is symmetrical as well.

Since the linear equations originating in Eq. (11) are homogeneous, $\gamma_1, \gamma_2, \ldots, \gamma_N$ can be obtained to make the determinant of the matrix $\left(\overline{A} + \gamma \overline{B}\right)$ equal to zero.

Once the eigenvalues, γ_n, have been determined the values of coefficients d_{nj} corresponding to γ_n can be obtained. Again, since the simultaneous equations resulting from Eq. (11) are homogeneous, one of the coefficients d_{nj} can be selected arbitrarily to be equal to 1 without any loss of generality. Therefore, for a specified d_{nj}, a system of (N-1) equations should be solved by obtain $d_{n2}, d_{n3}, \ldots, d_{nN}$.

To obtain coefficients C_n in Eq. (6) the initial condition given by Eq. (3a) is used. Then, when t = 0, from Eq. (6) we get:

$$\Phi^*\left(r^*,z^*\right) = \sum_{n=1}^{N} C_n \Psi_n\left(r^*,z^*\right) \tag{13}$$

By multiplying both sides of Eq. (13) by $f_i \; dV^*$ and by integrating over the volume of the solid, we obtain

$$\int_{V^*} f_i \Phi^*\left(r^*,z^*\right) dV^* = \int_{V^*} \sum_{n=1}^{N} f_i C_n \Psi_n\left(r^*,z^*\right) dV^* \tag{14}$$

The results of Eq. (14) will be a set of N linear algebraic equations that allows determination of

$C_1, C_2, \ldots, C_n$. This completes the solution of the problem.

The average value of the variable Φ^* is given by (Whitaker, 1980):

$$\overline{\Phi^*} = \frac{1}{V^*}\int_{V^*} \Phi^*\left(r^*, z^*, t^*\right) dV^* \tag{15}$$

where V^* is the volume of the solid being studied.

In this work the GBI method was used to solve the problem of mass transport inside spheroidal solids (prolate spheroid, oblate spheroid and sphere). In this case, $\Phi = M$ (moisture content), $\Gamma^{\phi} = D$ (diffusion coefficient) and λ=1. Fig. 1 illustrates an ellipsoid of revolution. The contour of the solid is defined by

$$\frac{x^2}{a^2} + \frac{y^2}{a^2} + \frac{z^2}{b^2} = 1 \tag{16}$$

Since $r^2 = x^2 + y^2$, Eq. (16) can be written as follows:

$$z = b\sqrt{1 - \left(\frac{r}{a}\right)^2} \tag{17}$$

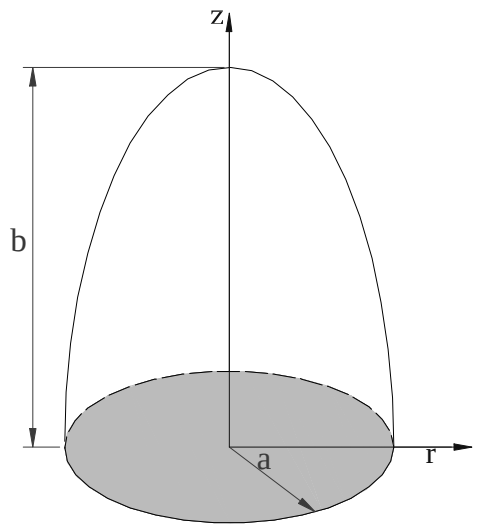

Figure 1: Ellipsoid of revolution and characteristics.

Thus, the following initial and boundary conditions can be given as follows:

$$M(r, z, t = 0) = M_0 = cte \tag{18a}$$

$$M\left(r = a, z = \sqrt{1 - \left(\frac{r}{a}\right)^2}, t\right) = M_e \tag{18b}$$

$$\frac{\partial M}{\partial z} = 0 \text{ for r = 0, for every t;} \tag{18c}$$

$$\frac{\partial M}{\partial r} = 0 \text{ for z = 0, for every t} \tag{18d}$$

Using the dimensionless parameters defined in Eqs. (4a-e), we have

$$z^* = \frac{b}{a}\sqrt{1 - \left(r^*\right)^2} \tag{19}$$

and the initial and boundary conditions in dimensionless form are:

$$M^*\left(r^*, z^*, t^* = 0\right) = 1 \tag{20a}$$

$$M^*\left(r^* = 1, z^* = \frac{b}{a}\sqrt{1 - \left(r^*\right)^2}, t^*\right) = 0 \tag{20b}$$

$$\frac{\partial M^*}{\partial z^*} = 0 \text{ for r = 0, for every t;} \quad (20c)$$

$$\frac{\partial M^*}{\partial r^*} = 0 \text{ for r = 0, for every t} \quad (20c)$$

The base functions, f_j, are given by

$$f_j(r,z) = \left(1 - \frac{r^2}{a^2} - \frac{z^2}{b^2}\right) r^{(p-q)} z^q \quad (21)$$

or, in the dimensionless form as follows:

$$f_j\left(r^*, z^*\right) = \left[1 - \left(r^*\right)^2 - \frac{a^2}{b^2}\left(z^*\right)^2\right] a^p \left(r^*\right)^{p-q} \left(z^*\right)^q \quad (22)$$

where p = 0, 2, 4,..., NP and q = 0, 2, 4,...,p. In this work ten base functions, which correspond to NP = 6, where used. These base functions are not orthogonal; however, according to Payne et al. (1986), functions Ψ_n are orthogonal.

To calculate the area (S) and volume (V) of prolate and oblate spheroids, the following equations, can be used (Mohsenin, 1986):

$$S = 4\pi a\, b \left\{ \frac{a}{2b} + \frac{1}{2} \frac{\arcsin\left[\sqrt{-\left[\left(\frac{a}{b}\right)^2 - 1\right]}\right]}{\sqrt{-\left[\left(\frac{a}{b}\right)^2 - 1\right]}} \right\} \quad (23)$$

valid for b/a<1.0

$$S = 4\pi a\, b \left\{ \frac{a}{2b} + \frac{\ln\left[\frac{a}{b} + \sqrt{\left[\left(\frac{a}{b}\right)^2 - 1\right]}\right]}{2\sqrt{\left[\left(\frac{a}{b}\right)^2 - 1\right]}} \right\} \quad (24)$$

valid for b/a>1.0

$$V = \frac{4}{3}\pi a^2 b \quad (25)$$

Eq. (25) is valid to prolate and oblate spheroid including sphere and circular disk. The Eqs. (23) - (25) were used to verify the effect of the shape of the solids on the drying kinetics. Other details about this formulation can be found in Farias (2002).

RESULTS AND DISCUSSIONS

Validation

To obtain the results, a computational code written in the Mathematica® language, version 4.1 was implemented (Wolfram, 1999). To validate the methodology presented here, some results are shown in Fig. 2 on the dimensionless moisture content at the center of the spheroid $(r^* = 0, z^* = 0)$ as a function of the Fourier number obtained in this work, compared with results reported by Payne et al. (1986) for spheroids with the aspect ratios $b/a = 2.00$ (prolate spheroid) and $b/a = 0.50$ (oblate spheroid) and for $b/a = 1.00$ (sphere). Analysing Fig. 2, a perfect agreement between the three cases presented can be observed.

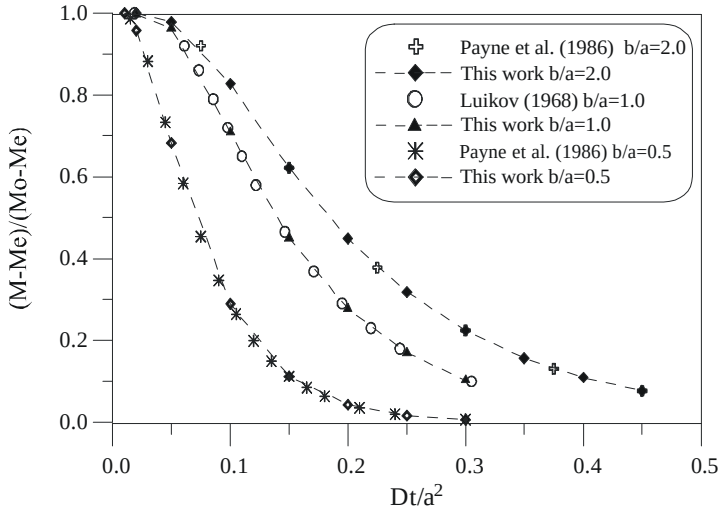

Figure 2: Moisture content in the center of three spheroids

Application

Using the model presented in this work, the behaviour of the dimensionless average moisture content can be traced for many spheroids as a function of Fourier number. Fig. 3 illustrates the dimensionless average moisture content of spheroids for aspect ratios that vary from b/a=0.25 to 5.00. Analysing Fig. 3, it can be observed that for the aspect ratio 0.25, the dimensionless average moisture content decreases much faster than for the aspect ratio 5.00. Therefore, it can be observed that the aspect ratio of the spheroid has a influence direct on the drying process. This is directly related to area/volume ratio (S/V). In a detailed analysis, it can be affirmed that the larger the area/volume ratio of a solid, the faster it will dry when maintained under the same experimental conditions.

Similar results were also observed in other work with oblate spheroids (Carmo, 2000) and prolate spheroids (Lima, 1999) as well as with other geometric forms, such as the parallelepiped (Nascimento, 2002). That characteristic is observed not only in the solids drying process, but also in heating, cooling and wetting processes.

In Figure 4 the dimensionless moisture content at the center of spheroids as a function of Fourier number is shown for several aspect ratios. Analysing this figure, it can be observed that the dimensionless moisture content at the center of the spheroid has the same behaviour as the dimensionless average moisture content in the previous illustration, so the smaller the aspect ratio the faster the loss of mass of the solid.

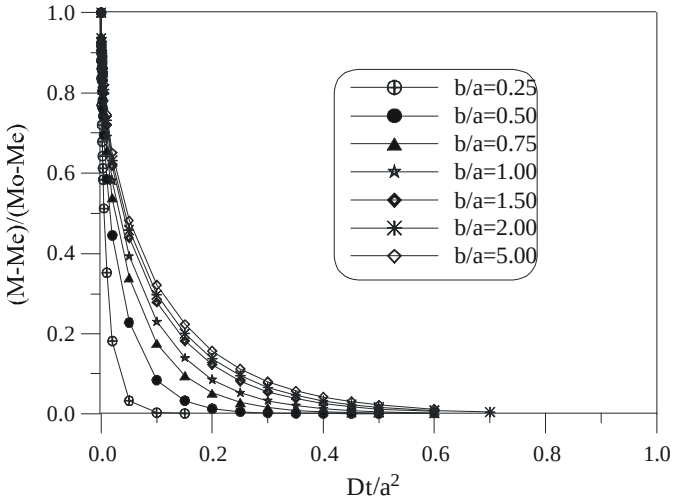

Figure 3: Dimensionless average moisture content as a function of Fourier number for several aspect ratios.

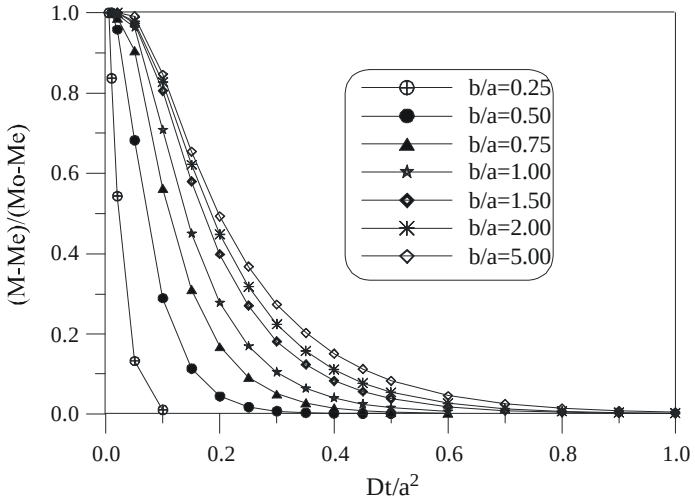

Figure 4: Dimensionless moisture content in the center of the spheroid as a function of the Fourier number for several aspects ratios.

It can be verified however that at the center of the spheroid, the behaviour of the curves is smoother than the behaviour of the curves of the dimensionless average moisture content. It can be concluded that the center of the spheroid is the place where the smallest moisture gradients are seen during the drying process for the same aspect ratio and the same Fourier number.

Figure 5 illustrates the behaviour of the dimensionless moisture content as a function of radial coordinate for several Fourier numbers for z*=0.0 for a spheroid with the aspect ratio $b/a = 0.5$. Analysing the illustration, it can be observed that the dimensionless moisture content decreases with the increase in Fourier number and radial coordinate.

Taking as reference the curve for the Fourier number $t^* = 0.05$ and $r^* = 0$, the value of the dimensionless moisture content is approximately 0.68 and for the coordinate $r^* = 0.8$, the value of the dimensionless moisture content is approximately 0.18. It can be observed that the dimensionless moisture content decreases with the increase in the coordinate r* for the same Fourier number, i.e., the closer to of the surface of the spheroid, the lower the dimensionless moisture content will be. This result shows that the moisture gradients are smaller close to the center of the spheroid and higher close to the surface, mainly for short times.

Figure 6 illustrates the behaviour of the dimensionless moisture content as a function of longitudinal coordinate for several Fourier numbers, for $r^* = 0$ for a spheroid with the aspect ratio $b/a = 0.5$. It can be observed that the curves have the same behaviour as the curves in Fig. 5; this demonstrates the dependence of the dimensionless moisture content of the longitudinal coordinate for any Fourier number. However, for the case presented in Fig. 5, it can be observed that the curves are smoother, with a variation in radial coordinate, indicating that the moisture gradients are larger in the direction of coordinate z*than in the direction of coordinate r* for a spheroid with the aspect ratio b/a=0.5.

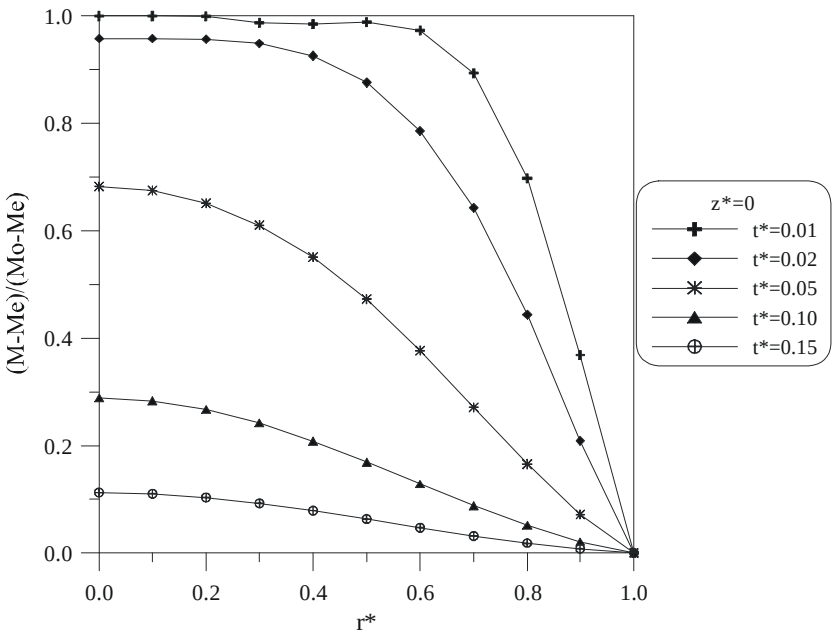

Figure 5: Dimensionless moisture content as a function of radial coordinate for several Fourier numbers for $z^* = 0$ for aspect ratio b/a=0.5.

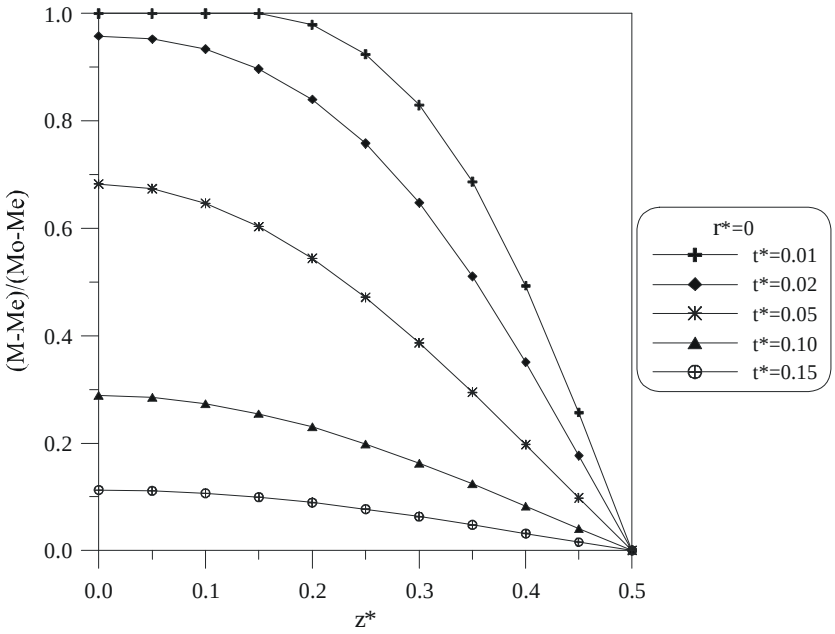

Figure 6: Dimensionless moisture content as a function of radial coordinate for several Fourier numbers for $r^* = 0$ for the aspect ratio $b/a = 0.5$.

In Figure 7 the behaviour of the dimensionless moisture content as a function of radial coordinate for several Fourier numbers for $z^* = 0$ is shown for a spheroid with the aspect ratio b/a=1.5 (prolate spheroid). Analysing the graph, it can be observed that the dimensionless moisture content depends on Fourier number and on coordinate r*, as expected, as in the case of oblate spheroids. So, it can be verified that, independent of the aspect ratio, the dimensionless moisture content depends directly on radial coordinate as well as on the Fourier number.

It can be noted that in Figures 5 and 7 for short times (t*=0.01) small mathematical oscillations occurred that didn't affect the results. Increasing the number of base functions can diminish this behaviour. Payne et al. (1986) compared the values of (1 - M*) with several numbers of base functions for ellipsoids with aspect ratios b/a = 0.5 and b/a = 1.5, where this effect is clearly observed.

In Figure 8 the dimensionless moisture content as a function of longitudinal coordinate z^* for several Fourier numbers for $r^* = 0$ for the aspect ratio $b/a = 1.5$ (prolate spheroid) is presented.

As in Fig. 7, the dependence of dimensionless moisture content on Fourier number and longitudinal coordinate is evident. It can be noted that the higher the Fourier number the smaller the dimensionless moisture content for the same coordinate r^* and/or z^*, so the higher the longitudinal coordinate the smaller the dimensionless moisture content for the same Fourier number and aspect ratio.

In Figures 9 and 10 the distribution of the dimensionless moisture content inside an oblate spheroid with the aspect ratio $b/a = 0.5$ as a function of the cylindrical coordinates (r^*, z^*) for elapsed times $t^* = 0.05$ and 0.10, respectively, is shown.

Analysing Fig. 9, it can be observed that the dimensionless moisture content distribution has high moisture gradients, mainly on the z^* axis and in proximity to the surface of the solid, as could already be seen in the Fig. 5. The iso-concentration lines are shown in the form of elliptic lines with the shape of an oblate spheroid. A phenomenon that occurs on the extremity of the spheroid in proximity to the coordinate $r^* = 1.00$ is observed; drying is quick in that area, generating high moisture gradients. Thus, this area is more susceptible to thermo-mechanical effects, such as cracking and deformation that could even rupture the solid. These effects jeopardise the quality of the product after drying. Several authors also reported this type of effect, for instance Lima (1999), Carmo (2000), Oliveira (2001), Nascimento (2002) and Oliveira and Lima (2002). The analyses in Fig. 10 demonstrate that the dimensionless moisture content distribution has low moisture gradients, i.e., the dimensionless moisture content distribution is already almost the same as that in the spheroid.

So, it can be verified that larger moisture gradients occur for lower Fourier numbers, tending to zero at the end of the process, when the solid reaches its dimensionless equilibrium moisture content.

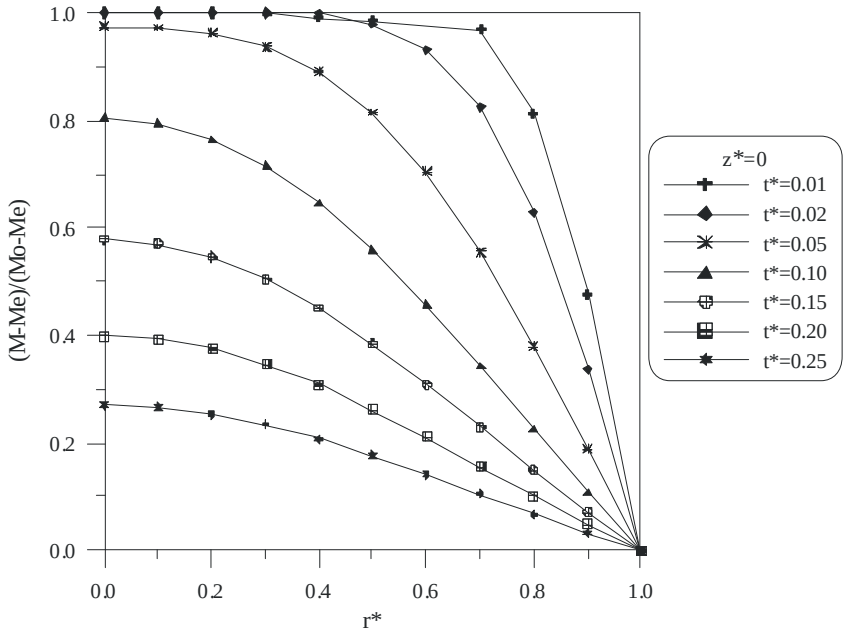

Figure 7: Dimensionless moisture content as a function of radial coordinate for several Fourier numbers for $z^* = 0$ for the aspect ratio b/a=1.5.

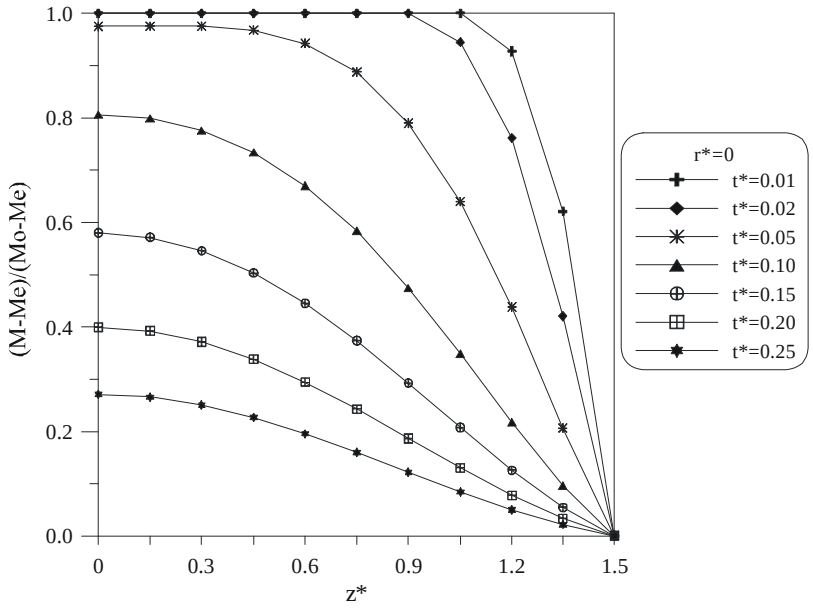

Figure 8: Dimensionless moisture content as a function of longitudinal coordinate z^* for several Fourier numbers for $r^* = 0$ for the aspect ratio $b/a = 1.5$.

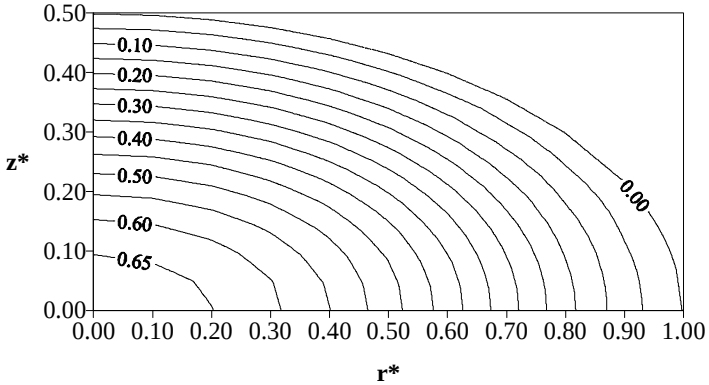

Figure 9: Distribution of the dimensionless moisture content for $b/a = 0,5$ and $t^* = 0.05$.

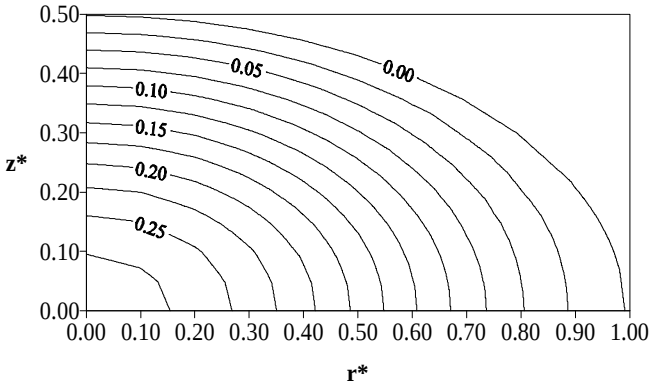

Figure 10: Distribution of the dimensionless moisture content for $b/a = 0.5$ and $t^* = 0.10$.

Figures 11 and 12 show the dimensionless moisture content distribution in a spheroid with the aspect ratio $b/a = 1.0$ (sphere) as a function of cylindrical coordinates for the Fourier numbers $t^* = 0.05$ and 0.10, respectively. Analysing Fig. 11, it can be noted that high moisture gradients are found in the spheroid, i.e., in the area close to the surface, the spheroid is practically dry, while at the center it is very moist. The iso-concentration lines are circular in the shape of the spheroid according to boundary conditions used in this work. In Fig. 12 smaller moisture gradients than in the previous case (t*=0.05) are seen. This indicates that the moisture moves from the center of the solid to the surface of the same.

Figures 13 and 14 illustrate the dimensionless moisture content distribution in a spheroid as a function of cylindrical coordinates (r^*, z^*) with aspect ratio $b/a = 1.5$ (prolate spheroid) for $t^* = 0.05$ and 0.01, respectively.

In analysing Fig. 13 high moisture gradients can be observed in the spheroid for $t^* = 0.05$. It can be noted that the iso-concentration lines have an elliptic form with the shape of a prolate spheroid. Analysing Fig. 14, it can be seen that the dimensionless moisture content distribution in the spheroid has smaller moisture gradients than in the case for $t^* = 0.05$ (Fig. 13) due to the water loss.

By comparing Figs. 9-14, it can be seen, that the area/volume ratio directly influences the drying kinetics. The higher the area/volume ratio, the faster the solid will dry.

The areas where high moisture gradients are found are the areas with the largest loss of water. These areas also have high temperature gradients, so are more apt to experience thermal shocks and consequently cracks, fractures and deformations, which depending on intensity may affect the quality of the product.

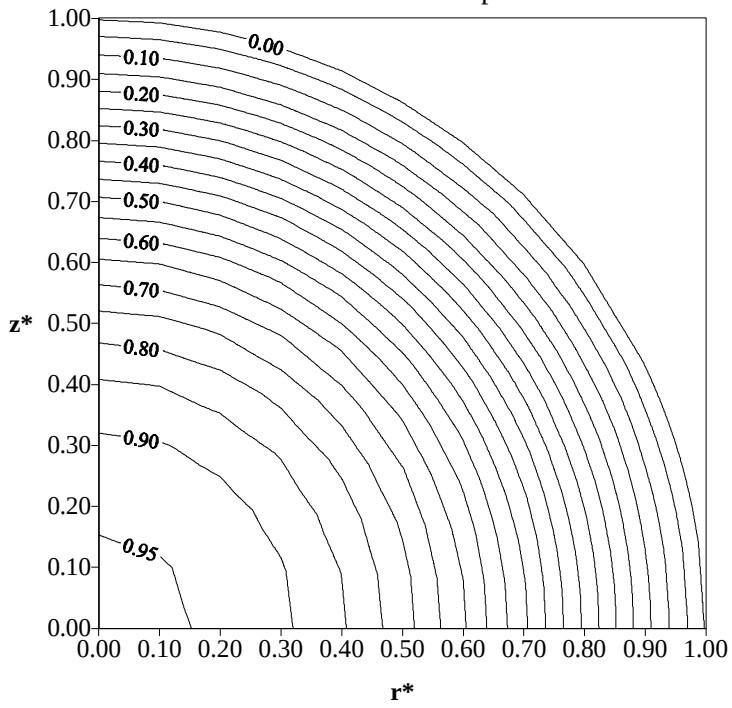

Figure 11: Distribution of the dimensionless moisture content for $b/a = 1.0$ and $t^* = 0.05$.

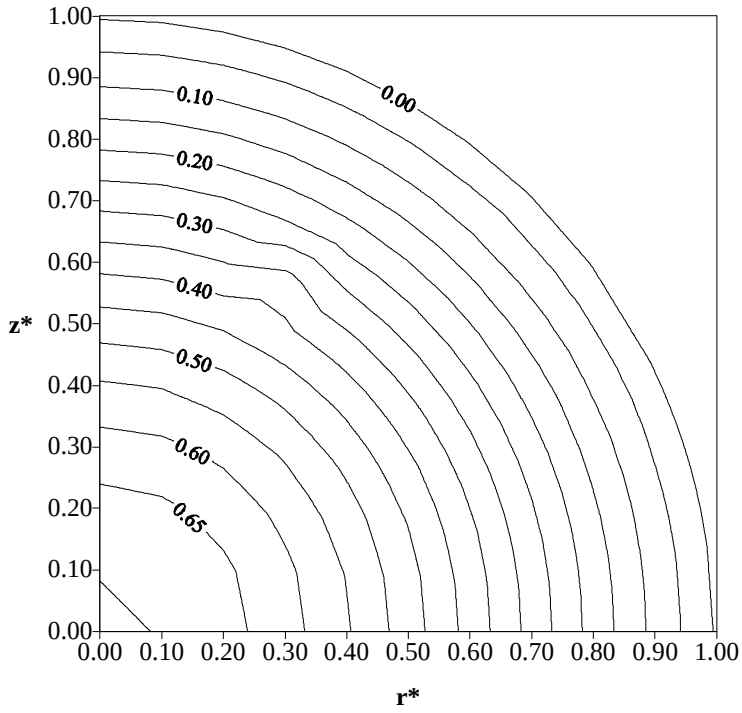

Figure 12: Distribution of the dimensionless moisture content for $b/a = 1.0$ and $t^* = 0.10$.

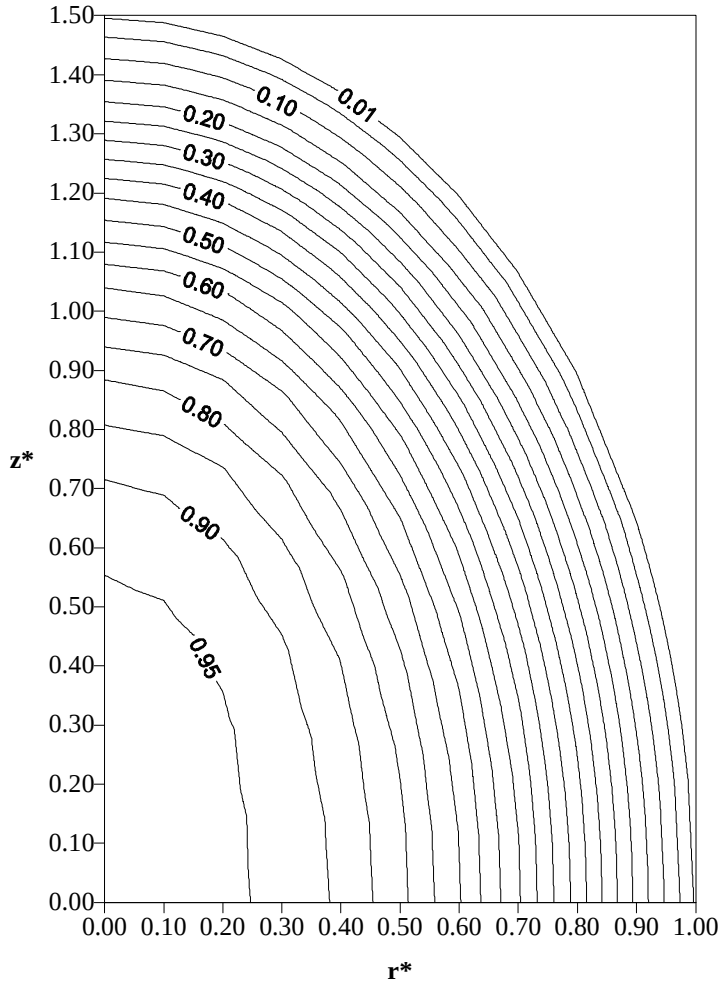

Figure 13: Distribution of the dimensionless moisture content for $b/a = 1.5$ and $t^* = 0.05$.

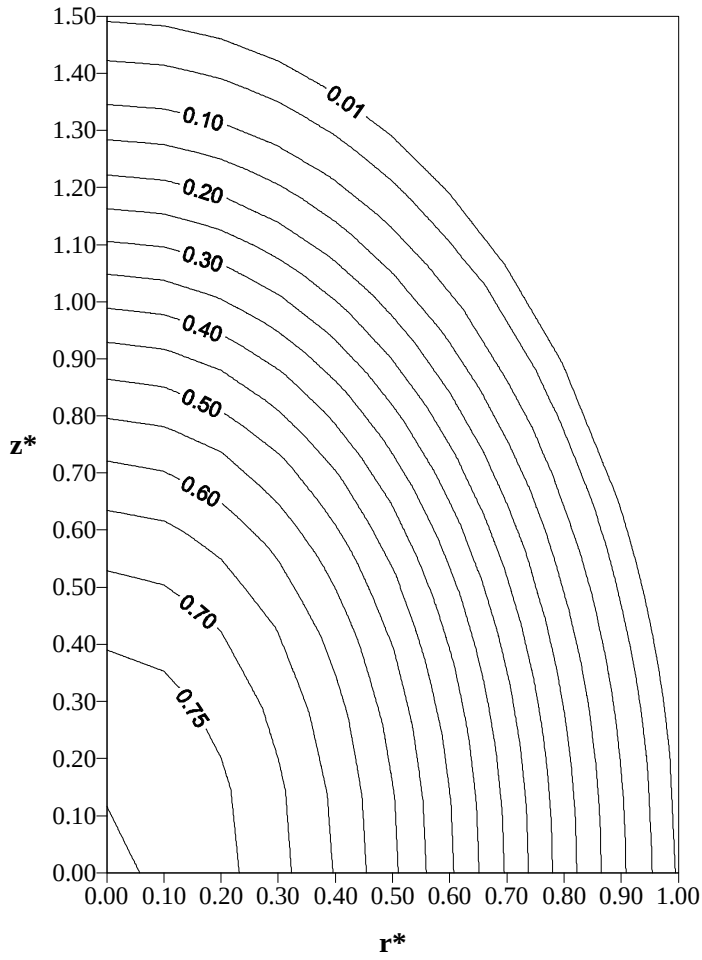

Figure 14: Distribution of the dimensionless moisture content for $b/a = 1.5$ and $t^* = 0.10$.

CONCLUSIONS

According to data obtained by simulation of the drying process in bodies with an ellipsoidal shape, it can be concluded that the mathematical modelling and the integral method based on Galerkin used to solve the problem of mass transport in solids that vary in shape from a circular disk to an infinite cylinder, including a sphere, was appropriate. The solution can also be used to describe other unsteady phenomena such as wetting, cooling and/or heating.

It was verified that the dimensionless average moisture content in a spheroid as well as the dimensionless moisture content at the center and at any point inside the same, it decreases with the increase in Fourier number for any aspect ratio. The form and aspect ratio of a spheroid directly influence the drying process, and this is directly related to the area/volume ratio, i.e., as the lower the area/volume ratio, the faster the drying for a fixed value of Fourier number.

During the drying process the smallest moisture gradients are found close to the center and the highest are found close to the surface, mainly for short times for any aspect ratio. The dimensionless moisture content depends on radial and longitudinal coordinates. The closer to the surface of the spheroid, the lower the dimensionless moisture content will be. The iso-concentration lines in the spheroid tend to have the same shape as the surface of the solid. This is due to the boundary condition used in this work. Oblate and prolate spheroids show a phenomenon called the tip effect, and the area with high moisture gradients is more significant in prolate spheroids.

ACKNOWLEDGEMENTS

The authors would like to express their thanks to CAPES (Coordenação de Aperfeiçoamento de Pessoal de Nível Superior, Brazil) and CNPq

(Conselho Nacional de Desenvolvimento Científico e Tecnológico), for their financial support of this work.

NOMENCLATURE

a, b	Characteristic dimensions	(m)
A_i,	Constant i = 0, 1, 2,....,n	(-)
$\bar{A}$, $\bar{B}$	Matrix N×N	(-)
C_n	Constants	(-)
D	Diffusion coefficient	($m^2 s^{-1}$)
d_{nj}	Constants	(-)
$\bar{d}_n$	Vector	(-)
$\partial M/\partial t$	Diffusion rate	(s^{-1})
f_j	Element of the set base function	(-)
g_n	Constants	(-)
M	Moisture content	(kg kg^{-1})
M_0	Initial moisture content	(kg kg^{-1})
M_e	Equilibrium moisture content	(kg kg^{-1})
$M^\bullet$	Dimensionless moisture content	(kg kg^{-1})
$\bar{M}$	Average moisture content	(kg kg^{-1})
$\bar{M}^\bullet$	Average dimensionless moisture content	(kg kg^{-1})
r	Radial coordinates	(m)
r^*	Dimensionless radial coordinates	(-)
$\vec{r}$	Vector	(-)
S	Area	(m^2)
t	Time	(s)
t^*	Fourier number	(-)
T	Temperature	(ºC)
V	Volume	(m^3)
V^*	Dimensionless volume	(-)
X, y, z	Cartesian coordinates	(-)
z^*	Dimensionless Cartesian coordinates	(-)

Greek Letters

∇	Gradient	(-)
∇^2	Laplacian	(-)
λ	Property of the solid	(-)
Φ	Physical parameters	(-)
Φ^*	Dimensionless physical parameters	(-)
$\bar{\Phi}^*$	Average dimensionless physical parameters	(-)
Φ'''	Source term of Φ	(-)
Γ^Φ	Transport coefficient	(-)
γ_n	n^{th} value	(-)
Ψ_n	Function	(-)
φ_n	Surface 1, 2, 3, ..., n	(-)
Σ	Sum	(-)

REFERENCES

Alassar, R. S., Heat Conduction From Spheroids. Journal of Heat Transfer, 121, No. 2, 497-499 (1999).

Beck, J.V., Cole, K.D., Haji-Sheikh, A. and Litkouhi, B., Heat Conduction Using Green's Functions. Hemispheric Publishing Corporation, New York (1992).

Carmo, J.E.F., Diffusion Phenomena in Oblate Spheroidal Solids: Modelling and Simulation, Master`s thesis, Federal University of Paraiba, Campina Grande (2000) (In Portuguese).

Carmo, J.E.F. and Lima, AG.B. Mass Transfer in Oblate Spheroidal Solids. 8th Brazilian Congress of Thermal Engineering and Sciences (ENCIT), Porto Alegre (2000).

Carmo, J.E.F. and Lima, A.G.B., Modelling and Simulation of Mass Transfer inside the Oblate Spheroidal Solids. 2nd Inter-American Drying Conference. Boca Del Rio, Vera Cruz, Mexico (2001).

Coutelieris, F.A., Burganos, V.N. and Payatakes, A. C., Convective Diffusion and Adsorption in a Swarm of Spheroidal Particles. AICHE Journal, 41, No. 3, 1122-1134 (1995).

Crank, J., The Mathematics of Diffusion. Oxford Science Publications, New York (1992).

Elvira, C., The Diffusion Process Modelling in Elliptic Shaped Bodies. International Congress Engineering and Food, v. 1, London (1990).

Farias, S.N., Drying of Spheroidal Solids Using the Galerkin Method. Master`s thesis, Federal University of Paraiba, Campina Grande (2002) (In Portuguese).

Feng, Z. and Michaelides, E.E., Unsteady Heat and Mass Transfer from a Spheroid, AICHE Journal. 43, No. 3 (1997).

Fortes, M., A Non-equilibrium Thermodynamics Approach to Transport Phenomena in Capillary-porous Media with Special Reference to Drying of Grains and Foods. Ph.D. Thesis, Pardue University (1978)

Gebhart, B., Heat Conduction and Mass Diffusion. McGraw-Hill, Inc., New York (1993).

Haghighi, K., Irudayaraj, J., Stroshine, R.L. and

Sokhansanj, S., Grain Kernel Drying Simulation Using the Finite Element Method, Transaction of the ASAE, 33, No. 6, 1957-1965 (1990).

Haji-Sheikh, A. and Sparrow, E.M., Transient Heat Conduction in a Prolate Spheroidal Solid, Transactions of the ASME: Journal of Heat Transfer, 88, No. 3, 331-333 (1966).

Igathinathane, C. and Chattopadhyay, P.K., Surface Area of General Ellipsoid Shaped Food Materials by Simplified Regression Equation Method, Journal of Food Engineering. 46, 257-266 (2000).

Lima, A.G.B., Diffusion Phenomenon in Prolate Spheroidal Solids. Case Study: Drying of Banana. Ph.D. Thesis. State University of Campinas, Campinas (1999). (In Portuguese).

Lima, A. G. B. and Nebra, S.A., Theoretical Analysis of the Diffusion Process Inside Prolate Spheroidal Solids, Drying Technology, 18, No. 1-2 (2000).

Lima, A.G.B., Queiroz, M.R. and Nebra, S.A., Heat and Mass Transfer Model Including Shrinkage Applied to Ellipsoids Products: Case Study: Drying of Bananas, Developments In Chemical Engineering And Mineral Processing, 10, No. 3-4, 281-304 (2002a).

Lima, A.G.B.; Nebra, S.A. and Queiroz, M.R., Simultaneous Moisture Transport and Shrinkage During Drying of Solids with Ellipsoidal Configuration, Chemical Engineering Journal, 86, No. 1-2, 85-93 (2002b).

Lu, R. and Siebenmorgen, T.J., Moisture Diffusivity of Long-grain in Rice Components, Transactions of the ASAE, 35, No. 6, 1955-1961 (1992).

Luikov, A.V., Analytical Heat Diffusion Theory. Academic Press, Inc. Ltd., London (1968)

Mohsenin, N.N., Physical Properties of Plant and Animal Materials. Gordon and Breach Publishers, Australia (1986).

Nascimento, J.J.S., Transient Diffusion Phenomenon in Parallelepipeds Solids. Case Studied: Drying of Ceramic Materials. Ph.D. Thesis, Federal University of Paraiba, João Pessoa (2002), (In Portuguese).

Oliveira, V.A.B., Diffusion in Prolate Spheroidal Solids: An Analytical Solution, Master`s thesis, Federal University of Paraíba, Campina Grande (2001), (In Portuguese).

Oliveira, V.A.B. and Lima, A.G.B., Unsteady State Mass Diffusion in Prolate Spheroidal Solids: An Analytical Solution. 2nd Inter-American Drying Conference. Boca Del Rio, Vera Cruz, Mexico (2001).

Oliveira, V.A.B. and Lima, A.G.B., Mass Diffusion Inside Prolate Spherical Solids: An Analytical Solution. Revista Brasileira de Produtos Agroindustriais, Campina Grande -Paraíba, 4, No. 1, 41-50 (2002).

Payne, F.R., Corduneanu, C.C., Haji-Sheikh, A. and Huang, T., Integral Methods in Science and Engineering. Chapter: On Solution of Parabolic Partial Differential Equations Using Galerkin Functions. Hemisphere Publishing Corporation, New York (1986).

Sarker, N.N., Kunze, O.R. and Stroubolis, T., Finite Element Simulation of Rough Rice Drying. Drying Technology, 12, No. 4, 761-775 (1994).

Sheen, S. and Hayakawa, K., Parametric Analysis for Frozen Spheroidal (Prolate and Oblate) or Finitely Cylindrical Food. Journal of Food Science, 57, No. 1, 236-248 (1992).

Whitaker, S., Advances in Drying. Chapter two: Heat and Mass Transfer in Granular Porous Media. vol. 1, Hemisphere Publishing Corporation, New York (1980).

Wolfram, S., The Mathematica® Book. Cambridge University Press, New York, 1999, 1403p.